African Journal of Applied Research
Vol. 9, No. 2 (2023), pp. 12-34
http://www.ajaronline.com
http://doi.org/10.26437/ajar.31.10.2023.02

OPTIMISATION OF PROCESS PARAMETERS ON COMPRESSIVE STRENGTH OF 3D-PRINTED POLYLACTIC ACID PARTS

Akpakpavi, M. K.[1], Sackey, S. M.[2], and Asante-Afrifa, M. K.[3]

[1] *Department of Mechanical Engineering, Accra Technical University, Accra, Ghana.*
[1, 2 & 3] *Department of Mechanical Engineering, Kwame Nkrumah University of Science and Technology, Kumasi, Ghana.*
[1]*micakpakpavi@yahoo.com*

ABSTRACT

Purpose: The purpose of this work is to optimise the influence of 3D printing processing parameters on the ultimate compressive strength of 3D-printed polylactic acid (PLA) parts. The objective is to develop the predictive models to help predict and attain optimized compressive strength integrity of 3D printed parts.

Design/Methodology/Approach: In the present study, 3D printed PLA samples were modelled and fabricated using carefully selected processing parameters-processing speed, processing temperature and nozzle diameter. Compressive tests were performed by ASTM D695-15 standard. Two characteristics response optimisation models based on the Taguchi Technique and multi-linear regression models were developed to optimize the process parameters and the ultimate compressive strength of the 3D printed samples.

Findings: Results of this study reveal that ultimate compressive strength is significantly affected by the Nozzle diameter. The ultimate compressive strength of the 3D-printed PLA sample was found to be significantly higher than the strength of the original PLA filament printed.

Research Implications/Limitations: In this study, only three critical 3D printing processing parameters including, processing speed; processing temperature and nozzle diameter were implemented concurrently.

Practical implication: By optimising process parameters, such as layer thickness, infill density, printing speed, and processing temperature, manufacturers can produce 3D-printed PLA parts with higher compressive strength. This leads to higher product quality and reliability.

Social implication: It can empower local communities and small businesses to manufacture parts and products that meet their specific needs. This can reduce dependence on centralized manufacturing and promote economic self-sufficiency.

Originality / Value: In this work, Nozzle diameter, which is a not too much studied 3D printing processing parameter, is implemented simultaneously with processing speed, and processing temperature to 3D print PLA filament to achieve an ultimate compressive strength value significantly higher than the strength of the original filament.

Keywords: *Compressive. experimental. optimisation. strength. 3D Printing.*

ISSN: 2408-7920

African Journal of Applied Research
Vol. 9, No. 2 (2023), pp. 12-34
http://www.ajaronline.com
http://doi.org/10.26437/ajar.31.10.2023.02

1.0 INTRODUCTION

3D printing is one of the most widely used additive manufacturing (AM) processes which can produce complex geometrical parts from a digital file (Shakeri et al., 2021; Ahmadifar et al., 2021; Maisarah et al., 2019). In 3D printing, objects are created using additive manufacturing, instead of subtractive manufacturing processes (Sumalatha et al., 2021). In an additive process, objects are created by laying down successive layers of material which forms a thinly sliced cross-section of the object (Mohammed, 2019).

Currently, 3D printing as a manufacturing method, is being used in diverse applications, instead of conventional techniques employed in modern manufacturing (Gomez-G et al., 2018). This is principally due to the numerous advantages that 3D printing offers compared to conventional energy-intensive manufacturing techniques including the ability to fabricate complex geometries as a single unit/part with no joints, lower material and labour cost, lower energy demand, single-step processing temperature, less process complexity (CAD model-print-install), quick production time, short lead time, the less overall cost compared to the conventional technologies, relatively less expensive moulds and tooling requirements, possibility to produce small batches or batches of one economically, enabling mass customisation, and so forth (Mohammed et al., 2020). More so, provided the 3D printing process is controlled, parts with good surface finish and near-net shapes can be produced (Chamil et al., 2020).

Challenges still exist across many AM processes (Brischetto et al., 2020). For example, a new foundation for CAD systems is needed that overcomes the limitations of solid modelling in representing very complex geometries and multiple materials. Presently, Significant variations in geometry and properties of 3D printed parts, and a limited availability of processable materials are some key challenges of 3D printing (Gibson et al., 2010). Again, the problem arises when the mechanical strength of a 3D printed part is compromised; it is a must for some 3D printed products to meet the specified quality of strength including compressive strength, and other mechanical and thermal properties (Lay et al., 2019). These need to be controlled to make the 3D printing process on the whole more efficient, effective, reliable and economical by saving time, material and post-processing operations without sacrificing the quality of the product (Ventola, 2014). Using different materials and printers with different combinations of controlled inputs, it is possible to define the quality of surface, mechanical, thermal and other properties of a 3D printed machinery part/component on different slopes. Also, currently, in the literature, not enough and sufficient work or research has been done to find out or predict the mechanical properties, typically, the compressive strength integrity of 3D printed parts using a combination of nozzle diameter, processing speed and temperature as combined processing parameters simultaneously and concurrently.

Therefore, among other things, the overall purpose of this study is to evolve a methodology that can be used to vary the pertinent process parameters for the 3D printing process to ensure optimized mechanical strength integrity. Ultimately, by performing this research, the quality of a

ISSN: 2408-7920

African Journal of Applied Research
Vol. 9, No. 2 (2023), pp. 12-34
http://www.ajaronline.com
http://doi.org/10.26437/ajar.31.10.2023.02

3D-printed PLA component or part can be predicted by establishing the relationship between the printing technique and the printing parameters which have a direct effect on the quality of printed products produced.

2.0 FUSED DEPOSITION MODELLING

Among the numerous additive manufacturing (AM) techniques, Fused Deposition Modelling (FDM) is the most popular: it is conceptually simple, does not pose a danger to health, and most of all the printing apparatus is cheap and of small tabletop size. Fused deposition modelling was developed by S. Scott Crump, co-founder of Stratasys, in 1988. The basic functioning of FDM is illustrated in Figure 1 (Kiński & Pietkiewicz, 2018): In general, the FDM process can be described as follows: first, the STL file is created from the 3D CAD model, then G-code is generated in a slicer software (Tlegenov et al., 2017). The functioning process of FDM printing starts with heating the liquefier to the desired temperature to melt the thermoplastic filament. After heating the filament, the melt is then extruded through a nozzle and then deposed layer-wise on a heated table, following a pattern calculated by the printer control software that will reproduce the desired geometry of the object, which can be input as a CAD file, typically in Stereo Lithography interfaces format (Rahman et al., 2015; Uz et al., 2019).

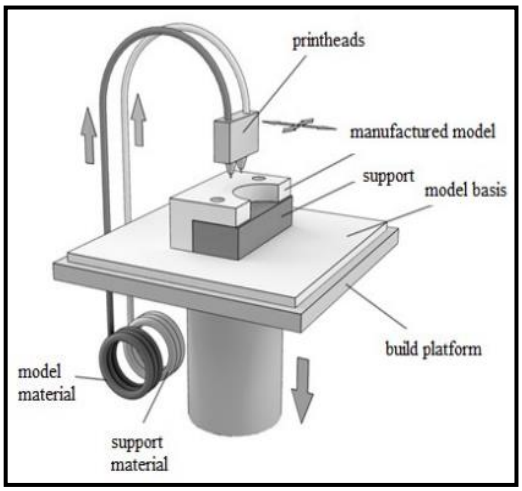

Figure 1: Schematic representation of FDM setup

Moreover, the FDM printing process depends on a large number of parameters, which are listed and briefly described in Table 1 (Valentina et al., 2019). For simplicity, the parameters can be grouped into three macro-categories, namely: extruder–related; process-related; and structural parameters.

ISSN: 2408-7920

African Journal of Applied Research
Vol. 9, No. 2 (2023), pp. 12-34
http://www.ajaronline.com
http://doi.org/10.26437/ajar.31.10.2023.02

Table 1: Description of the 3D-printing process parameters

Parameters		Description
Extruder Geometry	Nozzle diameter	Size of the exit orifice of the extruder
	Filament diameter	Size of the filament required by the extruder
Processing	Melt temperature	Temperature of the molten material exiting, the extruder
	Hot plate temperature	Surface temperature of the workpiece plate
	Printing speed	The velocity of the material deposition
Structural	Layer thickness	The thickness of the layer deposited by the nozzle
	Infill geometry	The internal structure of the printed component
	Infill density	Material percentage filling the component apparent vol.
	Number of layers	Number of shells deposed
	Raster angle	The angle between the deposed material and the X-axis
	Raster gap	The distance between two contiguous paths on the same layer
	Raster width	Width of the deposited material
	Patterning	Path followed to deposit the material on the workspace

Source: Valentina et al (2019)

Fused Deposition Modeling (FDM) technology needs to be improved in terms of geometrical stability, part quality, product strength and performance. A proper understanding of the processes and their traits is crucial to overcome these limitations (Sood, 2011). A significant amount of importance is given to the mechanical strength of RP fabricated parts as the mechanical properties are considered to be the most important indices for evaluating the fabrication quality of the process. The Necessity for research Design freedom, usage of less expensive tooling and moulds, and the subsequent removal of many designs for manufacture (DFM) related constraints help designers to adjust their design intent to facilitate component or assembly to be manufactured using the capability of 3D-printing. Manufacturing of different components simultaneously and sequentially, especially for low-volume production, is possible. Additive manufacturing is somewhat a fast and to a larger extent a flexible manufacturing technique with a reconfiguration capability. Consequently, its gains have benefited diverse fields like medicine, aerospace, automobile, construction, manufacturing, food, education, tooling and die making etc. (Hopkinson et al., 2006).

3.0 MATERIALS AND METHODS

3.1. Printing Material, 3D Printer, and Specimen Modelling and Preparation

In this work, pure Polylactic Acid Resins (PLA) of size 1.75 mm diameter, is used as the raw material for preparing the red samples for this work. The filament was purchased from Amazon and sold by 3D Bazaar. For this work, the PLA filament material used, according to the manufacturer has the following physical and mechanical properties as depicted in Table 2.

African Journal of Applied Research
Vol. 9, No. 2 (2023), pp. 12-34
http://www.ajaronline.com
http://doi.org/10.26437/ajar.31.10.2023.02

Table 2: Physical and Mechanical properties of the PLA used for this work according to the manufacturer

Property	Testing Method	Typical Value/ Printing	Typical Value/Injection molding
1. Tensile strength (MPA)	ASTM D638 (ISO 527)	49.5 ± 1.3	69.5 ± 0.50
2. Elongation at break (%)	ASTM D638 (ISO 527)	3.0 ± 0.4	28 ± 0.30
3. Bending modulus (MPA)	ASTM D790 (ISO 178)	3200 ± 220	3326 ± 210
4. Compressive strength (MPA)	ASTM D695 (ISO 527)	48.2 + 1.5	69.5 ± 0.5
5. Bending strength (MPA)	ASTM D790 (ISO 178)	92.1 ± 2.2	108.0 ± 12
6. Impact strength (KJ/m^2)	ASTM D256 (ISO 179)	3.4 ±0.21	4.0 ± 0.25
7. Density (g/cm^3)	ASTM D792 (ISO 1183)	2.36	
8. Glass Transition temperature	DSC.IO 'C/min	50-60	
9. Melting index (g/IO min)	I"C216 kg	5-7	
10. Color	-	Black, Red	

3.1.1 3D Printer

Craftbot IDEX Cartesian 3D printer, as indicated in Figure 2, is used in this research for producing the compressive specimens for this work. This printer has the capacity to 3D print materials such as: Polylactic acid (PLA), Acrylonitrile Butadiene Styrene (ABS), Polyvinyl Alcohol (PVA), High-density polyethylene (HDPE) and similar materials. The printer is located in the laboratories of the Intermediate Technology Transfer Unit (ITTU), Suame Magazine, Kumasi, affiliated with KNUST.

Figure 2: CraftBot IDEX Cartesian 3D printer, at the Intermediate Technology Transfer Unit (ITTU), Suame Magazine, Kumasi, affiliated with KNUST

ISSN: 2408-7920

African Journal of Applied Research
Vol. 9, No. 2 (2023), pp. 12-34
http://www.ajaronline.com
http://doi.org/10.26437/ajar.31.10.2023.02

3.1.2 Dimensions and Modeling of Compressive Test Specimen

The compressive test sample specimens used in this study are modelled based on ASTM D695 type–15 standards (ASTM International, 2014). Solidworks software is used for modelling the geometry of the compressive specimens as indicated in Figure 3, by the ASTM D695 standards. The ASTM D695-15, which is the Standard Test Method for Compressive Properties of Rigid Plastics, defines the standard test specimens for strength measurement as a form of a right cylinder whose length is twice its principal diameter. Accordingly, the preferred size is 12.7 mm in diameter by 25.4 mm in length (0.50 by 1 inch). Solidworks software is used for modelling the geometry of the compressive specimens as per the standards. The Model is then saved in .stl file format, and then imported to the 3D printing software.

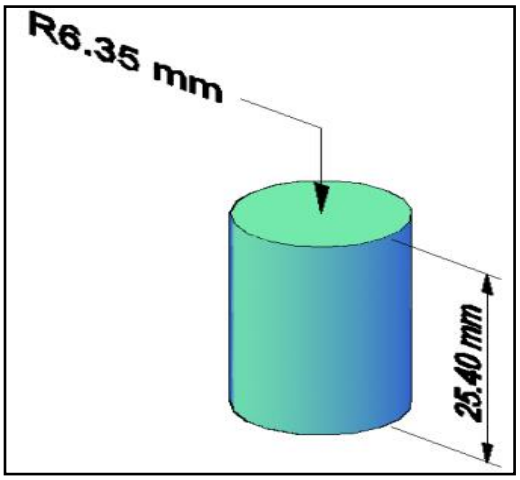

Figure 3: Compressive test specimen with dimension

3.1.3 Specimen Fabrication

The compressive test specimens fabricated in this work, have the same shape and geometrical dimensions as shown in figure 3. The 3D printer used to fabricate the compressive samples is pictured in Figure 2. Among the tools used for the measurement of the prepared samples chiefly include, permanent marker, and digital calipers. The 3D printed PLA specimens were subsequently conditioned at a temperature of 23℃, and for forty (40) hours before proceeding with the compressive tests as per the ASTM standards (ASTM International, 2014).

3.2 Experimentation

The research design is based on experimentation and the following procedures are discussed in the following sections.

3.2.1 Taguchi's Approach to Parameter Design

Taguchi's approach to parameter design enables engineers to systematically and efficiently optimise design parameters for performance and cost (Raviteja, et al., 2020; Durakovic, 2017;

ISSN: 2408-7920

African Journal of Applied Research
Vol. 9, No. 2 (2023), pp. 12-34
http://www.ajaronline.com
http://doi.org/10.26437/ajar.31.10.2023.02

Mohammed et al., 2019). The main steps in the Taguchi approach for parameter design include: (1) Determine the quality characteristics to be optimised; (2) Identify the Noise factors and test conditions; (3) Identify the control factors and their alternative levels; (4) Design the matrix experiment and define the data analysis procedure; (5) Conduct the matrix experiment; (6) Analyze the data and determine optimum level of control factors; (7) Predict the performance at these levels (Wille, 1990).

3.2.2 Optimum Levels Determination using the Taguchi Method

To analyze the results of experiments, and to obtain the optimal test parameter after investigations, the Taguchi method, which uses a statistical measure of performance called signal-to-noise (S/N) ratio borrowed from electrical control theory is used. The S/N ratio model developed by Dr. Taguchi is a performance measure to choose control levels that best cope with noise (Atefeh, et al. 2021).

In this work, compressive strengths of the 3D-printed PLA parts are required to be maximized and optimised, hence, the *Biggest-is-best characteristic* is the required ratio to be used for this work. Subsequently, equation 1, applies.

- *Biggest-is-best quality characteristic (strength, yield),*
  $S/Nratio\ (\eta) = -10\log_{10}\left(\frac{1}{n}\ ?_{i=1}^{n}\ \frac{1}{y_i{}^2}\right)$ **(1)**
- *Smallest-is-best quality characteristic (contamination),*
  $S/Nratio\ (\eta) = -10\log_{10}\left(\frac{1}{n}\ ?_{i=1}^{n}\ y_i{}^2\right)$ **(2)**
- *Nominal-is-best quality characteristic (dimension).*
  $S/Nratio\ (\eta) = -10\log_{10}\left(\frac{\mu^2}{\sigma^2}\right)$ **(3)**

3.2.3 Analysis of Variance (ANOVA)

Analysis of Variance (ANOVA) is a hypothesis-testing method used to analyze the equality of two or more population (or treatment) means by examining the variances of samples which are taken. ANOVA permits us to determine whether the differences between the samples are only due to random error or if there are systematic treatment effects which make the mean in one group differ from the mean in another. Mainly, ANOVA is used to compare the parity of three or more means, but when the means from two samples are compared using ANOVA, it is similar to using a t-test to compare the means of independent samples (Krishnaiah, et al., 2012).

3.2.4 Optimum Condition Predictions Using ANOVA Approach

In this work, the objective is to maximize the compressive strength and to predict its strength value as a response. For the factors involved in this work, i.e., the processing speed (S), the processing

African Journal of Applied Research
Vol. 9, No. 2 (2023), pp. 12-34
http://www.ajaronline.com
http://doi.org/10.26437/ajar.31.10.2023.02

temperature (T) and the nozzle diameter (D), the predicted optimum response is obtained using equation (4) (Krishnaiah et al., 2012):

$$\mu_{predict} = \bar{Y} + (\bar{S}_1 - \bar{Y}) + (\bar{T}_1 - \bar{Y}) + (\bar{D}_1 - \bar{Y})$$
$$= (\bar{S}_1 + \bar{T}_1 + \bar{D}_1) - 2\bar{Y} \quad \textbf{(4)}$$

3.3. Optimum Condition Predictions Using Multi-Regression Analysis

In experiments, if the response (Y) is linearly related to more than one independent variable, the relationship is modelled as multiple linear regression. Suppose, we have X_1, X_2, X_3…. X_k independent variables (factors). A model that might describe the relationship is as presented in equation 5 (Krishnaiah, et al., 2012):

$$Y = \beta_0 + \beta_1 X_1 + \beta_2 X_2 + \beta_k X_k + e \quad \textbf{(5)}$$

3.3.1 Hypothesis Testing in Multi-linear Regression

The test for significance of regression is to determine whether there is a linear relationship between the response variable Y and the regression variables X_1, X_2, X_3 ….X_k.

H_0: $\beta_1 = \beta_1$ .....…… $\beta_k = 0$
H_1: $\beta_j = 0$ for at least one j. **(6)**

Rejection of H_0 implies that at least one regression variable contributes to the model. The test procedure involves ANOVA and F-test (Krishnaiah et al., 2012).

3.4 Process Parameters Selection and Their Limits

In this work, a not much-studied process parameter, nozzle diameter, is used simultaneously with other process parameters including processing speed, and processing temperature to evaluate their concurrent and instantaneous effect on 3D-printed PLA materials in terms of compressive strengths.

Three levels of parameters are considered for sample preparation in this work, and the parameters which are kept constant throughout this experimentation are shown in Tables 3 (a, b) respectively.

Table 3a: Factors and their levels for this work

Factor	**Symbol**	**Unit**	**Level**		
			Low level (I) (-1)	**Centre point (0)**	**High level (+1)**
Processing speed	S	mm/s	70	80	90
Processing temperature	T	℃	215	220	230
Nozzle diameter	D	mm	0.40	0.60	0.80

ISSN: 2408-7920

African Journal of Applied Research
Vol. 9, No. 2 (2023), pp. 12-34
http://www.ajaronline.com
http://doi.org/10.26437/ajar.31.10.2023.02

Table 3b: List of fixed parameters used for this work

Parameter	Value
Filament diameter (mm)	1.75
Filament color	Red
Hot plate temperature (℃)	60
Layer thickness (mm)	0.2
Wall thickness	2.0 mm
Infill density	100%
Infill geometry	Linear
Layer height	Compute as per the relation above
Number of layers	2
Raster angle (°)	0
Speed while travelling (mm/s)	120
Part orientation	Flat

3.4.1 Experimental Design Based on the Taguchi Method

To evaluate the effect of printing parameters of the FDM process on PLA printed parts, in terms of compressive strength, a Taguchi method is used to optimise the process. In this work, experimental designs are carried out using Taguchi's L_9 Orthogonal Array (OA) experimental design which consists of 9 combinations of processing speed, processing temperature and filament diameter. It considers three process parameters (without interaction) to be varied in three discrete levels. The experimental design is presented in Table 4 of this report.

3.5 Compressive Experimental Test Procedure

3D-printed PLA specimens conditioned as per ASTM D695-15 for this work, are tested experimentally for compressive strength on a Pilot Control universal static compressive material testing machine, located in the laboratories of the Ghana Standard Authority, Legon, Accra. Figure 4 depicts the Pilot Control compressive testing machine used for testing the 3D-printed compressive PLA specimens for this work. A load of 5.0 kN at a constant speed of 5 mm/min is applied. Test specimens are prepared in compliance with ASTM D695-15 standard. Sample width and thickness are measured for individual specimens.

In the Versatile Automatic Pilot machine during testing, each specimen was placed between two compression platens installed in the materials testing machine. The machine crossheads moved the platens together with the specified 5.0 kN force. The failure at the end of the compression tests of the specimens in the machine was indicated by a sound signal and the results were captured on the data acquisition system of the instrument. Accordingly, the required compressive load for every specimen was captured. The mechanical properties to be obtained from the compressive tests for this work are as presented in equations (7-9).

ISSN: 2408-7920

African Journal of Applied Research
Vol. 9, No. 2 (2023), pp. 12-34
http://www.ajaronline.com
http://doi.org/10.26437/ajar.31.10.2023.02

$$S_y = \frac{F_{max}}{A_O} \quad (7)$$

$$S_U = \frac{F_{break}}{A_O} \quad (8)$$

$$\varepsilon_t = \frac{L}{L_O} \quad (9)$$

Where:

F_{max}: maximum compressive load,
F_{break}: the compressive force sustained by the specimen at breakage,
L_o: original grip separation,
L: extension (change in grip separation),
A_O: Original cross-sectional area.

Figure 4 pictures the Versatile Automatic Pilot PRO compressive testing machine used for the testing of the compressive samples in this work.

Figure 4: Versatile Automatic Pilot PRO compressive testing machine, at the Ghana Standard Authority Laboratories, Legon, Accra

4.0 RESULTS AND DISCUSSION

The results of the compressive test are captured in Table 4 of this report. The table shows the Taguchi L_9 orthogonal array. In all forty-five (45) red PLA samples were prepared and tested. As indicated in Table 4, there are nine experiment levels in all, hence, five representative samples were printed for each experimental level. Therefore, every experimental result value (that is, the ultimate compressive load (kN); ultimate compressive strength (N/mm^2), recorded in Table 4 for each of the nine experimental levels, is an average of five (5) tested samples to guarantee the reliability of test results. Figures 5 (a, b), illustrate a few of the compressive test samples before and after the compressive test procedures.

African Journal of Applied Research
Vol. 9, No. 2 (2023), pp. 12-34
http://www.ajaronline.com
http://doi.org/10.26437/ajar.31.10.2023.02

(a) (b)

Figure 5: Prepared PLA Compressive test samples (a) PLA test samples before testing and (b) deformed PLA test samples after compressive testing

4.1 Experimental Results and Taguchi Analysis

The results of the experiment are captured in Table 4 of this report. Subsequently, a table of signal-to-noise ratio (S/N) for ultimate compressive strength in this work is calculated for each experiment of L_9, essentially using equation 1 above. To calculate the S/N values in this work for the compressive tests, the Taguchi Orthogonal Array is designed in Minitab18, using the compressive test results table presented in Table 4 of this report. It can be seen clearly from Table 4 that for the compressive output response factors, the largest resultant ultimate Compressive strength value is (80.31 N/mm^2).

Moreover, for the S/N values presented in Table 4, graphs of the main Effects Plot for S/N ratios for ultimate Compressive strength, and Main Effects Plots for Means for the same ultimate Compressive strength) were plotted to determine the effects of 3D printing parameters on the Ultimate Compressive Strength of the 3D printed parts. The graphs plotted are as pictured in Figure 6 (a and b) respectively. Copiously, from the graphs, the optimal determined 3D printing parameter effects and their levels accordingly are: Nozzle Diameter (D) at level 3 (0.8 mm); Processing Speed (S) at level 3 (90 mm/s); and Processing Temperature at level 3 (230 ℃).

4.2 Analysis of Variance (ANOVA)

Table 5 and Figure 7 show the percent effect of each parameter on the Ultimate Compressive Strength (UCS) of the 3D-printed samples. It can be seen that the Nozzle Diameter (D) has the most significant effect on the output response (UCS), and its contribution is 87.61%. After that, the second significant factor for the UCS is processing speed(s), and its contribution is about 11.38%, and the third significant factor for the UCS in this work is the Processing Temperature (T), with a contribution of about 0.39%.

4.3 Validation of Results

Validation of results is an important part of any experimental analysis and in project works like this. In this work, two Prediction Models, together with results confirmation experiments have

African Journal of Applied Research
Vol. 9, No. 2 (2023), pp. 12-34
http://www.ajaronline.com
http://doi.org/10.26437/ajar.31.10.2023.02

been established to help analyze, predict, validate and above all, optimize the Ultimate Compressive Strength of 3D-printed PLA parts. These predictive models include prediction by Taguchi Method and prediction by multi-linear regression Techniques. These techniques are therefore explained in the subsequent sections of this report.

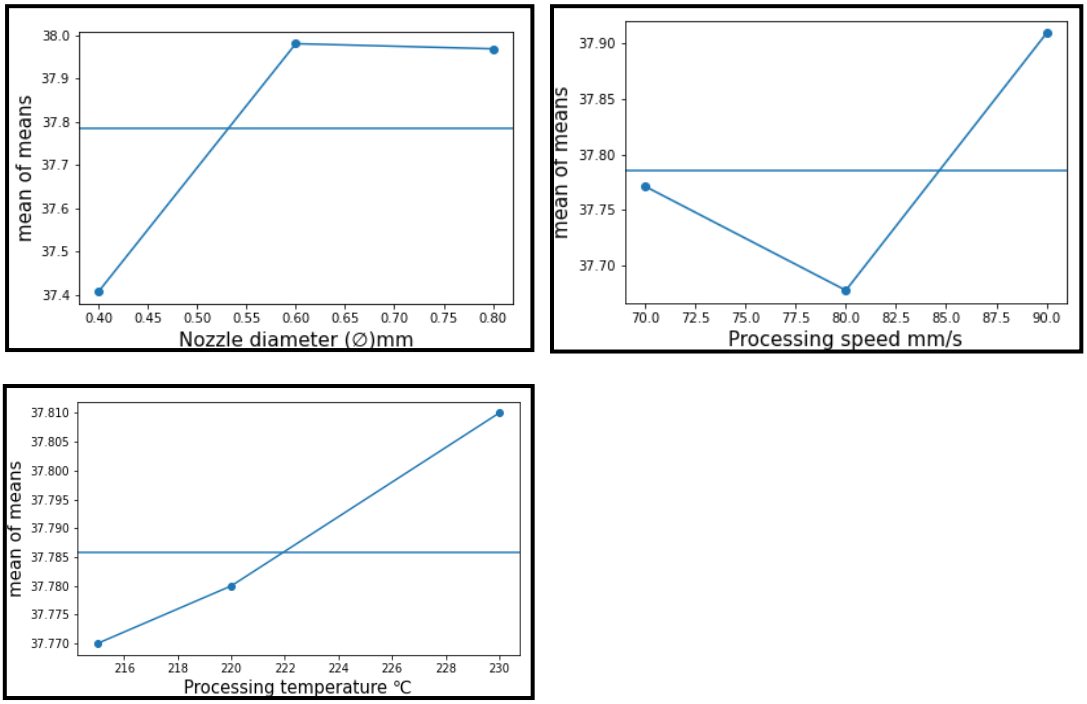

Figure 6(a): Main effects plot for S/N ratios (UCS)

ISSN: 2408-7920

African Journal of Applied Research
Vol. 9, No. 2 (2023), pp. 12-34
http://www.ajaronline.com
http://doi.org/10.26437/ajar.31.10.2023.02

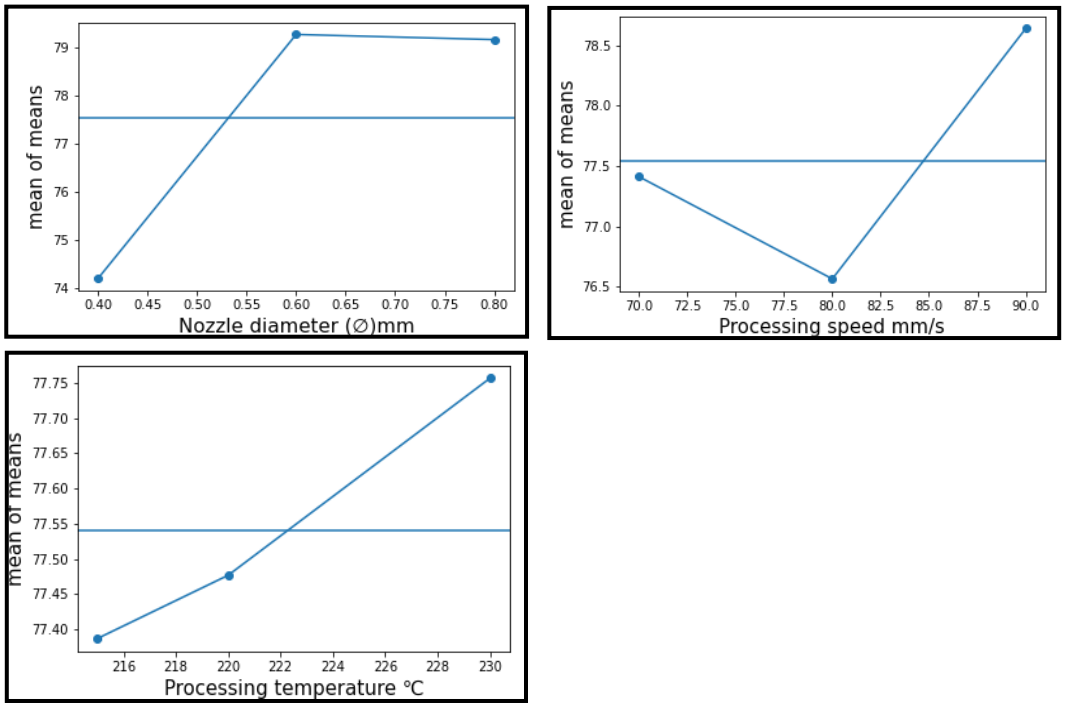

Figure 6(b): Main effects plot for means (UCS)

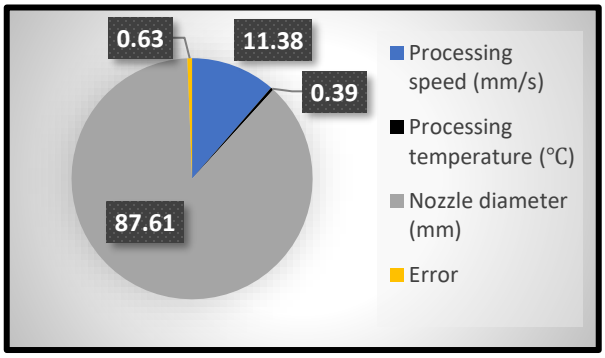

Figure 7: Significance of process parameters for Ultimate Compressive Strength

4.4 Prediction by Taguchi Method

For the optimal condition of process parameters, as determined in section 4.1 of this report: Nozzle Diameter (D) at level 3 (0.8 mm), Cutting Speed (S) at level 3 (90 mm/s), Processing Temperature (T) at level 3 (230 °C), the value of the optimised Ultimate Compressive Strength can be predicted according to equation 4.1 (Krishnaiah et al., 2012).

African Journal of Applied Research
Vol. 9, No. 2 (2023), pp. 12-34
http://www.ajaronline.com
http://doi.org/10.26437/ajar.31.10.2023.02

Ultimate Compressive Strength (UCS) $_{predict}$ = $(\bar{D}_3 + \bar{S}_3 + \bar{T}_3) - 2\bar{Y}$ **(10)**

Hence using the parameter levels stated in Table 3:

$$\bar{Y} = \frac{73.65+79.28+79.31+78.20+77.85+73.65+80.31+75.30+80.31}{9}$$

$$\underline{\bar{Y} = 77.54} \quad \textbf{(11)}$$

$$\bar{S}_3 = \frac{80.31 + 75.3 + 80.31}{3}$$

$$\underline{\bar{S}_3 = 78.64} \quad \textbf{(12)}$$

$$\bar{T}_3 = \frac{79.31+73.65+80.31}{3}$$

$$\underline{\bar{T}_3 = 75.62} \quad \textbf{(13)}$$

$$\bar{D}_3 = \frac{79.31+77.85+80.31}{3}$$

$$\underline{\bar{D}_3 = 79.16} \quad \textbf{(14)}$$

Hence, the Calculated Optimised Ultimate Compressive Strength (UCS) value using the Taguchi Model is as given:

UCS $_{predictive}$ = $(\bar{D}_3 + \bar{S}_3 + \bar{T}_3) - 2\bar{Y}$

UCS $_{predictive}$ = 79.16 + 77.76 + 78.64 – (2 x 77.54)

UCS = 80.48 N/mm^2 **(15)**

ISSN: 2408-7920

African Journal of Applied Research
Vol. 9, No. 2 (2023), pp. 12-34
http://www.ajaronline.com
http://doi.org/10.26437/ajar.31.10.2023.02

Table 4: Ultimate Compressive Experimental Results and Corresponding S/N Ratio

Experiment Number	Processing speed	Processing temperature	Nozzle Diameter (Ø)	Average ultimate compressive load (F)	Average ultimate compressive strength(σ)	S/N Ratio Ultimate compressive strength
	mm/s	℃	mm	kN	N/mm^2	
1	70	215	0.40	9.10	73.65	37.34345502
2	70	220	0.60	9.50	79.28	37.98327283
3	70	230	0.80	9.45	79.31	37.986559
4	80	215	0.60	8.76	78.20	37.86413506
5	80	220	0.80	9.70	77.85	37.82517234
6	80	230	0.40	9.02	73.65	37.34345502
7	90	215	0.80	9.70	80.31	38.09539252
8	90	220	0.40	8.98	75.30	37.53589952
9	90	230	0.60	8.72	80.31	38.09539252

Table 5: ANOVA for Average Ultimate Compressive Strength

Source	DF	SS	% Contribution	MS	F	P
Processing speed (mm/s)	2	6.52	11.38	3.2601	18.17	0.052
Processing temperature (℃)	2	0.22	0.39	0.1117	0.62	0.616
Nozzle diameter (mm)	2	50.22	87.61	25.1086	139.93	0.007
Error	2	0.36	0.63	0.1794		
Total	8	57.32	100.00			

4.5 Ultimate Compressive Strength Prediction by Multi-Linear Regression Analysis

Minitab 18 software is used to develop the Multiple Linear Regression Predictive Model for the Ultimate Compressive Strength (UCS) in this work. The predictors are: Processing Speed (S), Processing Temperature (T) and Nozzle Diameter (D).

The *Regression Equation* for ultimate compressive strength (UCS) for this work using the coefficients obtained in Table 6 is therefore fitted as:

$$\underline{\mathbf{UCS}} = 59.60 + 0.0613 \text{ Processing Speed (S)} + 0.025 \text{ Processing Temperature (T)} + 12.39 \text{ Nozzle diameter (D)} \quad \mathbf{(16)}$$

ISSN: 2408-7920

African Journal of Applied Research
Vol. 9, No. 2 (2023), pp. 12-34
http://www.ajaronline.com
http://doi.org/10.26437/ajar.31.10.2023.02

The significance of each coefficient in the UCS regression equation 16 above, was analyzed using ANOVA and tested by the p-value statistics, and by the method of model comparison. From Table 5, the regression statistics indicate that the coefficient for Nozzle Diameter (D) is statistically significant. That is, $p<0.05$ at a 95% confidence level. This therefore rejects the null hypothesis, since at least one of the parameters out of the three (processing speed, processing temperature and nozzle diameter) is significant. Hence, the stated linear regression model (equation 16) is valid, and therefore, there is a significant linear relationship between the input variables and the output results.

More so, Figures 8 (a, b, c) show the plot of standardized residuals versus fitted values, the plot of percentile versus standardized residuals, and the plots of Residuals versus observations respectively. From these graphs, it is inferred that the model is a good fit for the data.

Additionally, to compare the fixed multi-linear equation model with the ANOVA model established in section 4.4 of this report, an optimised UCS value was calculated by substituting the optimal condition of process parameters, Nozzle Diameter (D) at level 3 (0.8 mm); Processing Speed (S) at level 3 (90 mm/s); and Processing Temperature (T) at level 3 (230 ℃) into the multi-linear regression equation as stated:

$$\begin{aligned}\textbf{UCS} &= 59.60 + 0.0613 \text{ Processing Speed (S)} + 0.025 \text{ Processing Temperature (T)} \\ &\quad + 12.39 \text{ Nozzle diameter (D)} \\ &= 59.60 + 0.0618*(90) + 0.025*(230) + 12.39*(0.8) \\ &= 59.60 + 5.562 + 5.75 + 9.912 \\ &= \underline{\mathbf{80.82\ N/mm^2}} \end{aligned} \quad \textbf{(17)}$$

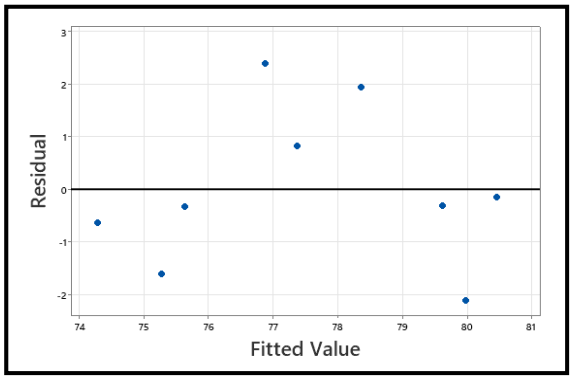

Figure 8 (a): Plot of standardized residuals vs. fitted value

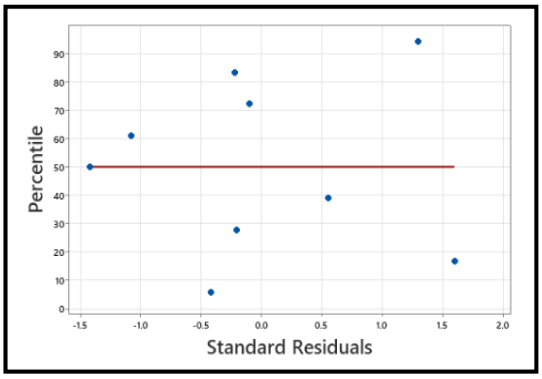

Figure 8 (b): Normal probability plot of Percentile vs. Standardized residuals

ISSN: 2408-7920

African Journal of Applied Research
Vol. 9, No. 2 (2023), pp. 12-34
http://www.ajaronline.com
http://doi.org/10.26437/ajar.31.10.2023.02

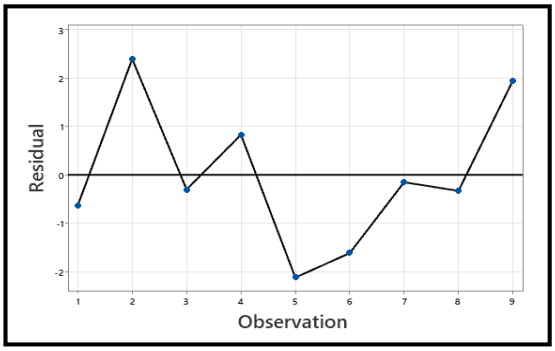

Figure 8 (c) Plot of Residuals vs. Observation

Table 6: Regression Table for Ultimate Compressive Strength (UCS)

Predictor	Coefficient	Standard Error Coefficient	T stat	P-Value
Constant	59.6	23.4	2.54	0.052
Processing speed (mm/s)	0.0613	0.0774	0.79	0.464
Processing temperature (℃)	0.025	0.101	0.25	0.814
Nozzle diameter (mm)	12.39	3.87	3.20	0.024

4.6 Confirmation of Compressive Strength Experiment Result

To validate the results obtained during the compressive strength experiments, it is necessary to perform confirmation experiments for the compressive strength response characteristics at optimal levels of the process variables, that is, Nozzle diameter (D) at level 3 (0.8 mm); Processing speed (S) at level 3 (90 mm/s); and Processing temperature at level 3 (230 ℃). The average value of the ultimate compressive strength characteristics from the confirmation tests was compared with the predicted values, as obtained in the previous sections of this paper. This average value is calculated in Table 7.

Table 7: Result of confirmation compressive test experiment

Experiment No.	Ultimate Compressive Strength (N/mm^2)
1	80.00
2	81.01
3	79.82
Average	80.28

ISSN: 2408-7920

African Journal of Applied Research
Vol. 9, No. 2 (2023), pp. 12-34
http://www.ajaronline.com
http://doi.org/10.26437/ajar.31.10.2023.02

4.7 Summary and Comparison of Optimal Predicted Values for the Two Models Developed in this work and the average value of the confirmation compressive test results

Table 8 presents the Ultimate Compressive Strength (UCS) of the optimal combination of process parameters by the two predictive Models developed in this work, and the confirmation compressive test experiment results (table 7). It can be seen from Table 8 that, the highest predicted value of UCS in this work (80.82 N/mm^2), obtained from the Multi-linear Regression Model, differs from the lowest predicted value by the Taguchi Method, by not so significant percentage value of 0.42%.

Also, the average Ultimate compressive strength (UCS) value from the confirmation experimental results (80.28 N/mm^2) as pictured in Table 8, differs by less than just 0.25% from the prediction by the Taguchi Model (80.48 N/mm^2).

Again, the approximate Optimised Ultimate Compressive Strength value of 81 N/mm^2 predicted by all two Predictive Models established in this work, which is approximately the same as the average Ultimate Compressive Strength confirmation experimental results (80.3 N/mm^2), tends to cross-validate the two models and demonstrate their significance. The two models (that is, the Taguchi model and multi-linear Regression models) established in this work, therefore, can be used to make meaningful, accurate, and relevant predictions of the Ultimate Compressive Strength of 3D-printed PLA parts.

Clearly, from the results obtained from this work, the optimised Compressive strength is about 81 N/mm^2, and this value is significantly influenced by the nozzle diameter with a contribution of about 87.61% of the three selected parameters and their levels used for this work. The nozzle diameters used for this work are: 0.4 mm, 0.6 mm and 0.8 mm; and the results are presented in section 4.2 of this report. The highest Compressive strength values are achieved at the highest selected nozzle of 0.8 mm. That is, as the nozzle diameter increases, the Compressive strength increases. Certainly, these findings from the work confirm the earlier works done by other authors. For example, according to Tezel and Kovan (2022), it is recommended to use a larger nozzle diameter and lower layer thickness to produce parts with superior properties. The study concluded that an increase in nozzle diameter leads to increased part strength, while layer thickness significantly affects surface quality. Increased nozzle diameter and part density contribute to reduced production time. It is recommended to use a larger nozzle diameter and lower layer thickness for parts with superior properties.

Also, Sukindar (2016), investigated the effect of nozzle diameter on the pressure drop, geometric error and extrusion time. The conducted analysis showed that the diameter of the nozzle and the processing speed have a significant influence on the pressure drop in addition to the plasticizing

ISSN: 2408-7920

African Journal of Applied Research
Vol. 9, No. 2 (2023), pp. 12-34
http://www.ajaronline.com
http://doi.org/10.26437/ajar.31.10.2023.02

Polymer chamber, which influences the consistency of the applied width of the path and, thus, the quality of the product finish.

Again, Czyzewski et al., (2022), examined the effects of the extruder's nozzle diameter on the improvement of functional properties of 3D-printed PLA products. In their experiment, the RepRap device for additive manufacturing was used, with the use of nozzles with diameters of 0.2 mm, 0.4 mm, 0.8 mm and 1.2 mm. The test samples were produced with a layer height of 0.2 mm, full filling (100%) and with constant remaining printing parameters. They reveal findings that, when it comes to strength properties, the samples produced with the use of nozzles with diameters of 0.4 mm and 0.8 mm were characterized by a higher Compressive strength. However, the lowest values of mechanical properties were observed in the case of samples produced with the use of the 0.2 mm nozzle. They also brought to the fore that, the use of an extruder nozzle diameter of 0.8 mm allows one to obtain a macrostructure with a high degree of interconnection of layers and paths and favourable mechanical properties. So, therefore, their test results can be used in the construction of functional elements that are produced by fused deposition modelling (FDM) and fused filament fabrication (FFF) methods in prototype, unit and small-lot production.

Table 8: Comparison of results (UCS)

Method	**Ultimate Compressive Strength (N/mm^2)**
Prediction by Taguchi Method	80.48
Prediction by Multi-linear Regression Analysis	80.82
Confirmation of Experimental UCS Results	80.28

5.0 CONCLUSI0N

In this work, the Optimisation of selected process variables including Processing speed, Processing temperature and Nozzle diameter on the compressive strength of 3D-printed PLA parts has been carried out according to the ASTM D695 standard. It was essentially done to determine, analyze and optimise the effects of the selected 3D printing process parameters at selected levels on the ultimate Compressive strength of 3D-printed PLA. The considered process parameters in this work are optimised to attain the maximum Compressive strength of the 3D-printed PLA parts. Taguchi's mean estimation method and a multi-linear regression model are used to predict the Ultimate Compressive strength of the 3D-printed PLA in this project. The following conclusion has been drawn from the study. Ultimate Compressive strength is mainly affected by Nozzle diameter (87.61%), and Processing speed (11.38%). The least significant parameter for Ultimate Compressive strength is processing temperature (0.39%). The best combination of process parameters for the 3D printing within the selected range is as follows: Increased Nozzle diameter at level 3 (0.8 mm), followed by Increased processing speed at level 3 (90 mm/s), and relatively increased Processing temperature at level 3 (230 ^{0}C). This, therefore, constitutes the determined optimal levels of the three selected 3D printing parameters used in this work.

ISSN: 2408-7920

African Journal of Applied Research
Vol. 9, No. 2 (2023), pp. 12-34
http://www.ajaronline.com
http://doi.org/10.26437/ajar.31.10.2023.02

Moreover, the Ultimate Compressive strength of the PLA filament used for this work according to the manufacturer and captured in Table 2 of this paper is around 48.2 N/mm^2. However, after 3D printing the red filament, using the selected parameters at their current selected levels, and performing the Compressive test experiments on the samples, the ultimate Compressive strength recorded was around 80.31 N/mm^2 (Table 4). This value, therefore, shows a significant improvement on the original ultimate Compressive strength of the PLA filament used for this work. This, among other things, suggests that with an informed and critical selection of process parameters, and implementing the same concurrently to 3D print PLA filaments, higher mechanical strength characteristics, including higher compressive strength properties are attainable. Indeed, observations and visits to most 3D printing industries, particularly in Ghana and elsewhere, reveal that 3D printing filaments are printed, using the same nozzle diameter without taking cognizance of the effects of the nozzle diameter on the mechanical, and thermal strengths of their 3D-printed products. Nonetheless, this research reveals that the nozzle diameter has the most profound effect on the compressive strength of the 3D-printed parts. It is, therefore, incumbent on 3D printing industries to select appropriate nozzle sizes to 3D print filaments to achieve desirable mechanical, thermal and surface finish properties.

5.1 Practical Implications

By optimising process parameters, such as layer thickness, infill density, processing temperature, printing speed, etc., manufacturers can produce 3D-printed PLA parts with higher compressive strength. This leads to higher product quality and reliability. It can reduce material wastage and improve material utilization. This is not only cost-effective but also environmentally friendly, as it reduces the amount of PLA filament required for production.

5.2 Social Implications

The optimisation of process parameters for 3D-printed PLA parts has social implications that encompass accessibility, education, sustainability, healthcare, disaster response, cultural preservation, and more. It represents a technology that can empower individuals, communities, and organizations to meet their specific needs and make a positive impact on society. The optimisation process as a whole, can also empower local communities and small businesses to manufacture parts and products that meet their specific needs. This can reduce dependence on centralized manufacturing and promote economic self-sufficiency.

Acknowledgement

Acknowledgement is to the Department of Mechanical Engineering of the Kwame Nkrumah University of Science and Technology, Kumasi, Ghana, for supporting this work.

ISSN: 2408-7920

African Journal of Applied Research
Vol. 9, No. 2 (2023), pp. 12-34
http://www.ajaronline.com
http://doi.org/10.26437/ajar.31.10.2023.02

6.0 REFERENCES

Ahmadifar, M., Benfriha, K., Shirinbayan, M., & Tcharkhtchi, A. (2021), Additive manufacturing of polymer-based composite using fused filament fabrication (FFF): A review. Appl. Compos. *Mater*. 28, 1335-1380.

ASTM International (2014), "Standard Test Method for Tensile Properties of Plastics: *U.S. Department of Defense*, Designation: D638-14".

Atefeh R. K., Saber R., Aliha, M. R. M, & Berto F. (2021). Optimization of properties for 3D printed PLA material using Taguchi, ANOVA and Multi-objective Methodology. *ScienceDirect, Elsevier*, 34(2021)71 - 77.

Bermudez, M. (2021). A theoretical and contextual background of 3D printing and design. *Novel Research in Sciences*, 7(1), 000654.2021.

Boon, W., & Van, W. B. (2018). Influence of 3D printing on transport: a theory and experts Judgement-based conceptual model. *Transport Reviews*, 38(5), 556-575.

Brischetto, S., & Torre, R. (2020). Tensile and compressive behaviour in the experimental tests for PLA specimens produced via fused deposition modelling technique. *Journal of Composite Science*, 4, 140, 40301140, 1-25.

Chamil, A., Pimpisut, S., & Anura, F. (2020). Optimization of Fused Deposition Modeling Parameters for Improved PLA and ABS 3D Printed Structures. *International Journal of Lightweight Materials and Manufacture*, 3(2020), 284-297.

Durakovic, B. (2017). Design of Experiments application, concepts, examples: state of the art. *Periodicals of Engineering and Natural Sciences*, 5, 2303 - 4521, 421-439.

Gibson, I., Rosen, D. W., & Stucker, B. (2010), "Additive Manufacturing Technologies: Rapid Prototyping to Direct Digital Manufacturing", *Springer*, New York, USA.

Gomez, G., Jerez-Mesa, R., Travieso-Rodriguez, J. A., & Liuma-Fuentes, J. (2018). Fatigue performance of fused filament fabrication PLA specimens. *Materials and desig*n, 140, 278-285.

Hopkinson, N., Hague, R., & Dickens, P. (2006). Rapid manufacturing: an industrial revolution for the digital age. *Wiley*, 9780470016138.

Imran, S., & Pushpendra, S. B. (2020). Reliability analysis of a 3D printing process. *ScienceDirect, Elsevier*, 173(2020), 1877-0509, 191-200.

Kinsk, W., & Pietkiewycz, P. (2019). Influence of the print layer height in FDM technology on the rolling height force value and the print time. *Sciendo*, 23(4), 2083-1587.

Krishnaiah, K., & Shahabudeen, P. (2012). Applied Design of Experiments and Taguchi Methods. *Asoke K. Ghosh, PHI Learning Private Limited*, New Delhi-110001, pp. 24-250

Lay, M., Thajudin, N. L. N., Hamid, Z. A. A., Rusli, A., Abdullah, M. K., & Shuib, R. K. (2019). Comparison of physical and Mechanical properties of PLA, ABS, and Nylon 6 fabricated using fused deposition modelling and injection molding. *Compos. Part B Engineering*, 176, 107341.

ISSN: 2408-7920

African Journal of Applied Research
Vol. 9, No. 2 (2023), pp. 12-34
http://www.ajaronline.com
http://doi.org/10.26437/ajar.31.10.2023.02

Maisarah, M., Mohamad, Z. M. O., & Mahfodzah, M. P. (2019). Optimization of 3D printing parameters for improving mechanical strength of ABS printed parts. *International Journal of Mechanical Engineering and Technology*, 10, 0976-6340, 255-260.

Mohammed, R. N., Garesh, B. K., & Madhan, P. (2019). Application of Taguchi's experimental design and range analysis in optimization of FDM printing parameters for PET-G, PLA and HIPS. *International Journal of Scientific and Technology Research*, 8(09), 2277 - 8616, 891-902.

Mohammad, D. Z. (2020). Study and characterization of Mechanical properties of wood-PLA composite (Timber fill) material parts built through fused filament fabrication. *Phd* thesis, *Universitat Politecnica De Catalunya*, Barcelonatech.

Pascucci, F., Perna, A., Runfola, A. & Gregori, G. L. (2018). The hidden side of 3D printing in management. *Symphoya, Emerging Issues in Management*. 2, 1593-0319, 91-107.

Rahman, K. M., Letcher, T., & Reese, R. (2015). Mechanical Properties of Additively Manufactured PEEK Components Using Fused Filament Fabrication; Proceedings of the Volume 2A: *Advanced Manufacturing, Proceedings of the IMECE2015*; Houston, TX, USA. 13–19.

Raviteja, B.V., Teja, A., Sarath, R. D., Sardeep, V., & Chandini, P. (2020). Optimization of cutting parameters in CNC turning machine using Taguchi method and ANOVA technique. *Journal of Engineering Technologies and Innovative Research*, 7, 2349-5162, 1277-1285.

Shakeri, Z., Benfriha, K., Shirinbayan, M., Ghodsian, N., & Tcharkhtchi, A. (2021). Modeling and optimization of fused deposition modelling process parameters for cylindricity control by using the Taguchi method. *International Conference on Electrical, computer, communications and Mechatronics Engineering* (ICECCME) 1-5.

Sood, A. K., Ohdar R. K., Mahapatra, S. S. (2012). Experimental investigation and empirical modelling of the FDM process for compressive strength improvement. *Journal of Advanced Research*. 3(1), 81-90.

Sukindar, N. A. (2016). Analyzing the effect of nozzle diameter in fused deposition modelling for extruding polylactic acid using open-source 3D printing. *J. Teknol*, 78, 7–15.

Sumalatha, M., & Malleswera, R. J. N. (2021). Optimization of process parameters in 3D printing-fused deposition modelling using Taguchi Method. *IOP Conference Series: Material Science and Engineering*, 1112(2021), 012009, 1-14.

Tlegenvo, Y., Wang, Y. S., & Hong G. S. (2017). A dynamic model for nozzle clog monitoring in fused deposition modelling. *Rapid Prototyping Journal*. 23, 391-400

Uz, Z., Boesch, U. K., Siadat, E., Rivette, A., & Baqai, M. (2019). Impact of fused deposition modelling (FDM) process parameters on the strength of built parts using Taguchi's design experiments of experiments. *In. J. Adv. Manuf. Technol.* 101, 1215-1226.

Valentina, M., Lorenzo M., & Francesco M. (June, 2019). FDM 3D printing of polymers containing natural fillers: A review of their mechanical properties. Polymers. 10, 3390, 11071094

Ventola, C. I. (2014). Medical Applications for 3D: Current and Projected Uses, *P T: Peer*

African Journal of Applied Research
Vol. 9, No. 2 (2023), pp. 12-34
http://www.ajaronline.com
http://doi.org/10.26437/ajar.31.10.2023.02

Rev.J. Formul. Manag., 39(10), 704-711.
Wille, R. (1990). Landing Gear Weight Optimization Using Taguchi Analysis, *Paper presented at the 49th Annual International Conference of the Society of Allied Weight Engineers Inc*, Chandler, AR.

ISSN: 2408-7920